ASEAN Journal for Science and Engineering in Materials

Journal homepage: https://ejournal.bumipublikasinusantara.id/index.php/ajsem

Numerical Investigation of Stress Concentration around Circular Holes in Functionally Graded Material (FGM) Plates Using the Extended Finite Element Method (XFEM)

*Huu-Dien Nguyen**

Nam Can Tho University, Can Tho City, Vietnam
*Correspondence: E-mail: nhdien@nctu.edu.vn

ABSTRACT

Stress concentration around circular holes is an important consideration in the mechanical design of functionally graded material (FGM) plates. This study investigates the effects of material gradation and hole interaction on stress concentration using the extended finite element method (XFEM) combined with a level-set approach. Isotropic and FGM plates containing single and interacting circular holes under uniaxial tensile loading were analyzed. The numerical model was validated against the classical analytical solution for an isotropic plate. The results demonstrated good agreement between numerical and analytical predictions. Material gradation significantly influenced stress concentration, while decreasing hole spacing increased stress concentration due to interactions between adjacent stress fields. These findings provide useful insights into the mechanical design and structural performance of perforated FGM plates.

© 2027 Bumi Publikasi Nusantara

ARTICLE INFO

Article History:
Submitted/Received 18 Jun 2026
First Revised 18 Sep 2026
Accepted 26 Oct 2026
First Available online 27 Oct 2026
Publication Date 01 Mar 2027

Keywords:
Extended finite element method;
Functionally graded material;
Level-set method;
Stress concentration factor;
Circular holes;
Hole interaction.

1. INTRODUCTION

Functionally graded materials (FGMs) have attracted considerable attention in engineering applications because their mechanical and physical properties can vary continuously within a structural component. Unlike conventional homogeneous materials, FGMs provide gradual transitions in material composition and properties, allowing their mechanical behavior to be adjusted according to specific structural requirements. Such characteristics make FGMs particularly suitable for engineering applications requiring improved stress distribution, structural reliability, and mechanical performance under external loading. The mechanical responses of functionally graded plates have been investigated using theoretical and numerical approaches, particularly in relation to deformation, stiffness distribution, and stress analysis [1, 2].

The mechanical behavior of engineering materials is closely related to their elastic properties and microstructural characteristics. Variations in crystallite size, microstructure, and material composition can influence mechanical properties, including elastic modulus and hardness. Experimental investigations of tungsten trioxide microparticles have demonstrated relationships between crystallite characteristics and micromechanical properties, highlighting the importance of material structure in determining mechanical responses [3, 4]. These relationships provide a broader understanding of the importance of material heterogeneity in mechanical engineering. In FGMs, spatial variations in elastic properties introduce additional complexity into stress redistribution, particularly when structural discontinuities are present [1, 2].

Circular holes are commonly introduced into engineering components for fastening, weight reduction, assembly, and functional requirements. However, the presence of holes produces local disturbances in the stress field, resulting in stress concentration around their boundaries. Excessive stress concentration can increase the susceptibility of structural components to localized damage and mechanical failure. The stress concentration factor (SCF) is therefore an important parameter for evaluating the mechanical performance of perforated plates. For homogeneous isotropic materials, the stress distribution around a circular hole under uniaxial tensile loading can be described using classical elasticity theory. However, the analysis becomes more complicated when the material properties vary spatially or when multiple holes interact within the same structural component [5].

Numerical methods have become important tools for investigating the mechanical behavior of materials and structures containing geometrical discontinuities. Conventional finite element methods (FEM) have been widely applied to stress and deformation analyses under various loading conditions. However, conventional FEM generally requires the computational mesh to conform to geometrical boundaries, which can increase the complexity of modeling irregular openings and changing geometrical configurations. The extended finite element method (XFEM) provides an alternative approach by introducing enrichment functions into the finite element approximation, allowing discontinuities and embedded boundaries to be represented without requiring complete remeshing. Previous investigations have demonstrated the applicability of XFEM and related numerical formulations to the analysis of cracks, holes, inclusions, and fracture characteristics in functionally graded materials [5-7].

Finite element approaches have also been employed in structural engineering to evaluate mechanical responses under external loading. Numerical investigations of reinforced

concrete structures have demonstrated the applicability of computational analysis to the assessment of structural deformation and mechanical performance. Although these applications involve different material systems and structural configurations, they illustrate the broader importance of numerical modeling in engineering analysis. For FGM plates containing circular openings, additional considerations are required because the spatial variation of elastic properties influences the stress field and its interaction with geometrical discontinuities [5-7].

Despite the development of numerical approaches for analyzing functionally graded structures, the combined effects of material gradation and interactions between circular holes remain important considerations in stress concentration analysis. The presence of adjacent holes modifies the surrounding stress distribution, while variations in material stiffness can further influence the magnitude and location of concentrated stresses. Consequently, the relationship between material gradation, hole spacing, and stress concentration requires systematic investigation. A numerical framework capable of representing circular openings and spatially varying material properties provides an appropriate approach for examining these coupled effects [5-7].

This study investigates stress concentration around circular holes in isotropic and functionally graded plates using XFEM combined with the level-set method. The analysis considers a single-hole configuration for numerical validation and extends the investigation to FGM plates and interacting circular holes. Particular attention is given to the effects of material gradation and hole spacing on the resulting SCF. The numerical approach is evaluated using an analytical solution for a single circular hole, while the interaction between adjacent holes is examined through numerical analysis and approximate analytical comparison. The findings are intended to improve understanding of stress redistribution in perforated FGM plates and provide useful considerations for the mechanical design of functionally graded structural components.

2. Theoretical Background

2.1. Functionally Graded Materials and Stress Concentration

The spatial variation of elastic properties is the defining characteristic of an FGM plate. Under elastic loading, changes in local stiffness influence the displacement field and redistribution of stresses around a void. The concentration factor is conventionally expressed as the ratio between the maximum local stress and the remote nominal stress. In graded plates, interpretation of this ratio requires the elastic-modulus distribution and the loading conditions to be specified consistently [1, 2, 5].

2.2. Analytical Stress Field around a Circular Hole

For a single circular opening of radius a in an infinite isotropic elastic plate subjected to remote uniaxial tensile stress, the Kirsch solution expresses the stress field in polar coordinates (r, θ). The radial, circumferential, and shear stress components are expressed in Equations (1), (2), and (3), respectively:

$$\sigma_r = \frac{1}{2}\sigma\left(1-\frac{a^2}{r^2}\right)+\frac{1}{2}\sigma\left(1-4\frac{a^2}{r^2}+3\frac{a^4}{r^4}\right)cos2\theta \quad (1)$$

$$\sigma_\theta = \frac{1}{2}\sigma\left(1+\frac{a^2}{r^2}\right)-\frac{1}{2}\sigma\left(1+3\frac{a^4}{r^4}\right)cos2\theta \quad (2)$$

$$\tau_{r\theta} = -\frac{1}{2}\sigma\left(1+2\frac{a^2}{r^2}-3\frac{a^4}{r^4}\right)sin2\theta \quad (3)$$

At the hole boundary (r = a), the maximum circumferential stress occurs at θ = 90° and 270° under uniaxial tensile loading. The corresponding theoretical SCF is 3.0, which serves as the analytical reference for validating the XFEM results for a homogeneous isotropic plate containing a single circular hole. This analytical solution is applicable to the isolated-hole configuration and does not directly describe the stress fields in functionally graded plates or plates containing interacting holes.

2.3. Level-Set Representation

The level-set method represents an embedded boundary using a scalar function whose magnitude corresponds to the shortest distance from a point x to the boundary Γ. The distance is assigned a positive sign in the material region and a negative sign within the void, while the zero level set defines the boundary itself. The signed-distance representation distinguishes the material and void regions through the sign convention illustrated in **Figure 1(a)**. The combination of level-set functions and XFEM enables holes and inclusions to be represented independently of the underlying finite element mesh, facilitating the numerical analysis of complex geometrical boundaries [8]. The signed-distance function is defined in Equation (4):

$$\phi(x) = \mp \min_{y \in \Gamma} |x - y| \tag{4}$$

The zero level set identifies the boundary, whereas negative and positive values represent the void and material regions, respectively. The sign convention is illustrated in **Figure 1(a)**, while **Figure 1(b)** presents the three-dimensional representation of the level-set function, showing the spatial variation of the function relative to the zero-level-set surface. Together, these representations illustrate how an embedded boundary can be described implicitly without requiring the computational mesh to conform to its geometry.

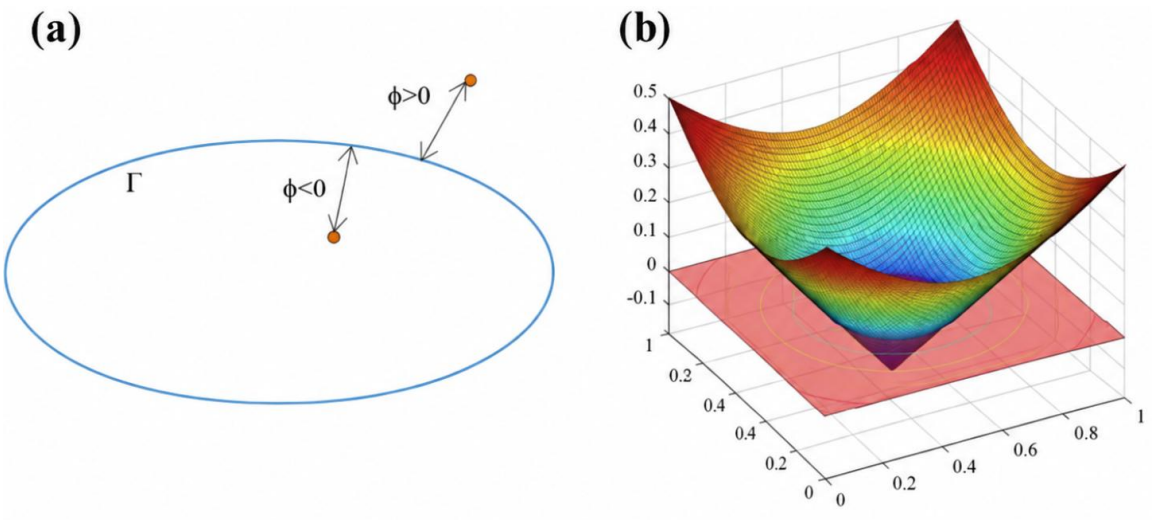


Figure 1. Schematic illustration of the level-set method: (a) definition of the level-set function with respect to the boundary Γ, where the function is negative inside and positive outside the domain; (b) three-dimensional representation of the corresponding level-set function.

For a circular boundary, the signed-distance function is expressed by Equation (5):

$$\phi = \|x - x_c\| - r_c \tag{5}$$

The circular boundary is defined by the hole-center coordinates and radius, as expressed in Equation (5). The level-set function is subsequently interpolated within each finite element using the corresponding shape functions and nodal level-set values, as expressed in Equation (6):

$$\phi(x) = N_i(x)\phi_i \tag{6}$$

Equation (6) describes the interpolation of the level-set function using finite element shape functions and nodal level-set values. For polygonal boundaries, the signed distance is evaluated by identifying the nearest boundary segment, determining the projection of the evaluation point onto that segment, and calculating the corresponding outward normal vector. The mathematical relationships defining these geometrical quantities are expressed in Equations (7)-(9):

$$\phi(x,0) = \|x - x_{min}\|\text{sign}\big((x - x_{min}).n_{min}\big), \tag{7}$$

$$\text{sign}(\xi) = \begin{cases} 1 & \text{if } \xi \geq 0, \\ -1 & \text{if } \xi < 0, \end{cases} \tag{8}$$

$$\|x - x_{min}\| = \min_{\substack{x_i \in I_i \\ i=1,2,\ldots,p}} \|x - x_i\|, \tag{9}$$

2.4. Fundamentals of XFEM Enrichment

The extended finite element method augments standard interpolation with enrichment functions. Thus, discontinuities or embedded interfaces can be represented independently of a globally conforming mesh [5, 6]. Enrichment-based finite element formulations enable discontinuities to be modeled without requiring continuous remeshing as their geometrical configurations evolve [9, 10]. The XFEM framework has also been extended to represent complex crack configurations, including branched and intersecting cracks, demonstrating the flexibility of enrichment functions in computational mechanics [11]. The indicator function distinguishing the material region and the void is specified in Equation (10):

$$V(x) = \begin{cases} 1 & \phi(x) > 0 \\ 0 & \phi(x) < 0 \end{cases} \tag{10}$$

The general XFEM fracture formulation includes crack-tip branch functions. The basis is given by Equation (11), where r and θ denote the local coordinates illustrated in **Figure 2(a)**:

$$\psi(x)|_{j=1}^{4} = \left(\sqrt{r}\sin\frac{\theta}{2}, \sqrt{r}\cos\frac{\theta}{2}, \sqrt{r}\sin\frac{\theta}{2}\sin\theta, \sqrt{r}\cos\frac{\theta}{2}\sin\theta\right) \tag{11}$$

The XFEM displacement approximation combines conventional nodal degrees of freedom and enrichment contributions, as expressed in Equation (12):

$$u(x) = \sum_{i\in I} N_i(x)u_i + \sum_{j\in J} N_j(x)H(x)a_j + \sum_{k\in K} N_k(x)\sum_{\alpha=1}^{4} F_\alpha(x)b_{k\alpha} \tag{12}$$

where *W* denotes all nodes, *H* identifies Heaviside-enriched nodes, and *T* identifies crack-tip enriched nodes. The branch functions represent the general crack-tip extension of XFEM, whereas the circular-hole treatment is based on the embedded void boundary. **Figure 2(b)** illustrates the representation of crack geometry using the level-set function, including the crack path, crack-tip location, and surrounding regions associated with the enrichment formulation.

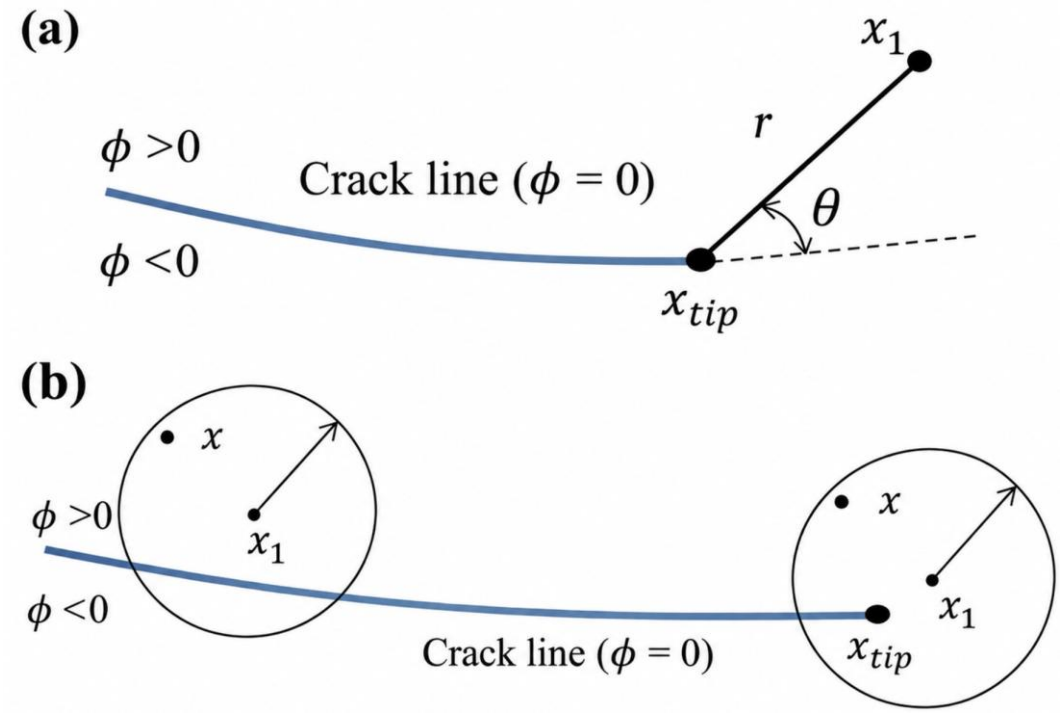


Figure 2. Schematic illustration of the level-set representation in XFEM: (a) local polar coordinates at the crack tip, including the radial distance (r) and angular coordinate (θ); (b) representation of the crack geometry using level-set functions and enrichment regions around the crack.

3. Materials and Methods

3.1. Numerical Research Framework

The analysis considered an isotropic single-hole benchmark, a single-hole FGM configuration and two-hole isotropic and FGM configurations. Geometry and material distributions were specified first; circular openings were described by level-set functions, and the stress field was evaluated through the numerical formulation. The SCF was then calculated and compared across the specified geometrical and material cases. The study sequence is summarized in **Figure 3**.

3.2. Geometry and Boundary Conditions

A thin elastic plate subjected to remote uniaxial tension in the x direction was considered. The first geometry consisted of a single circular hole, while the second comprised two equal circular holes aligned with the loading axis. The plate was described as linear elastic under plane-stress conditions. The single-hole and two-hole geometries are shown in **Figures 4(a) and (b)**, respectively. The complementary loading arrangement for a plate with a circular opening is depicted in **Figure 4(c)**.

For two identical circular holes of radius a separated by a center-to-center distance s, the normalized spacing ratio is defined by λ = s/(2a). The isotropic two-hole series considered λ = 1.05, 1.5, 2.0, 3.0, 4.0, and 6.0; the FGM two-hole series considered λ = 1.05, 1.5, 2.0, and 3.0.

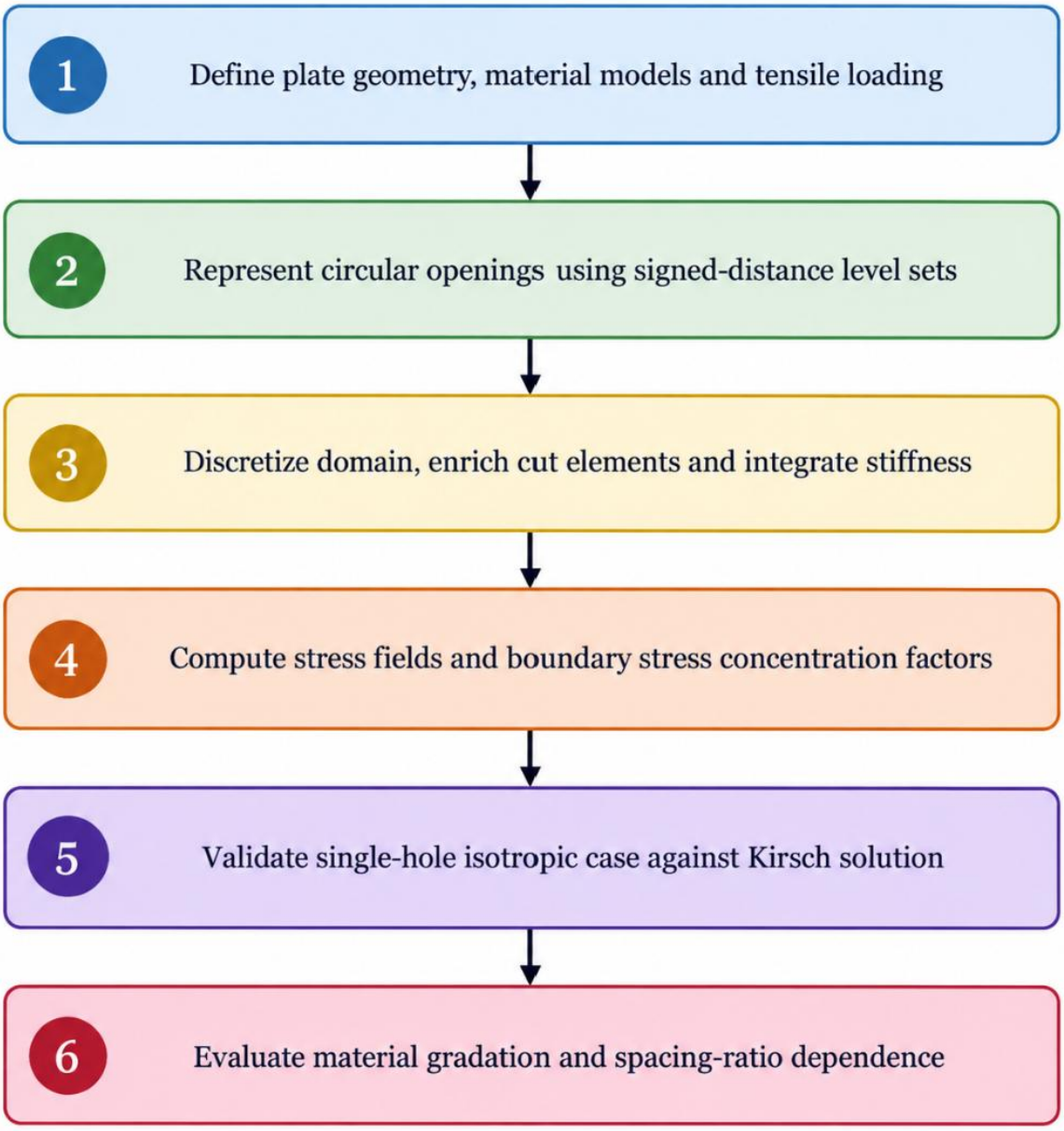


Figure 3. Numerical workflow for the stress concentration analysis of isotropic and functionally graded plates with circular holes.

3.3. Material Configurations and Grading Parameters

Homogeneous isotropic and functionally graded material (FGM) plates were investigated to evaluate the influence of spatial variations in elastic properties on stress concentration. In the isotropic configurations, the elastic properties were assumed to remain uniform throughout the plate. For the single-hole FGM configuration, the gradient indices were varied as n = 0, 1, 2, 5, and 10, whereas the two-hole FGM analysis considered n = 2, 5, and 10. An additional configuration involving a radially varying elastic modulus was examined for comparison with previous numerical results. The corresponding radial elastic-modulus distribution is expressed in Equation (13).

$$E_+(r) = E_o(1 - 0.5^{(r/r_o)}) \quad (13)$$

Equation (13) describes the radial distribution of the elastic modulus employed in the literature-comparison analysis. The parametric investigation of functionally graded plates was

conducted using material gradient indices of n = 0, 1, 2, 5, and 10 for the single-hole configuration and n = 2, 5, and 10 for the two-hole configuration. These gradient indices characterize the material-property variations considered in evaluating the influence of gradation on stress concentration.

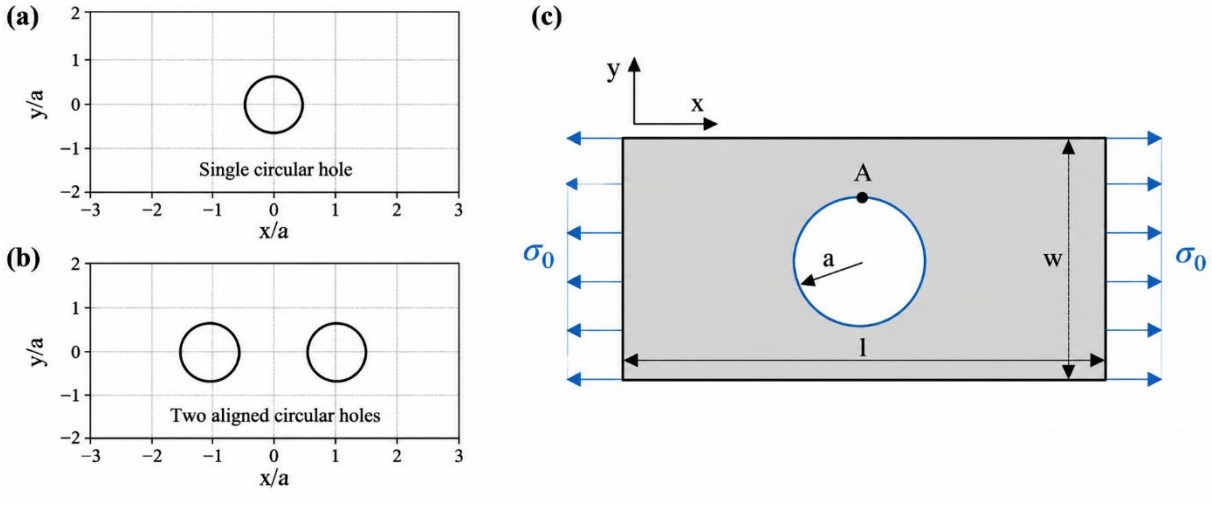


Figure 4. Geometrical configurations and loading conditions of plates containing circular holes: (a) single circular hole; (b) two horizontally aligned circular holes; and (c) rectangular plate with a central circular hole subjected to uniaxial tensile loading, showing the plate dimensions, hole radius, and applied stress.

3.4. XFEM Discretization and Integration

The level-set geometry was used to identify void and material regions and to locate elements intersected by the embedded boundary. The numerical procedure excludes degrees of freedom belonging to nodes inside the void. The numerical implementation of XFEM requires appropriate treatment of enrichment functions, element integration, and assembly of the discrete system to accurately represent discontinuities within the computational domain [12]. The cut or enriched elements are partitioned into integration subdomains using the zero-level-set boundary and Delaunay triangulation. Gaussian quadrature is then applied on the subdomains; second- or third-order quadrature schemes are considered for stiffness integration. **Figure 5(a)** illustrates the computational mesh containing embedded circular interfaces, while **Figure 5(b)** shows an enlarged view of an element intersected by the level-set boundary. The subdivision of the intersected element into triangular integration subdomains, including the positive and negative level-set regions and numerical integration points, is presented in **Figure 5(c)**. For an embedded circular void, the enriched-domain formulation is applied to the material side of the level-set boundary, and the stiffness contribution from void regions is excluded.

3.5. Stress Concentration Evaluation and Analytical Comparison

The stress concentration factor (SCF) was calculated as the ratio of the maximum circumferential stress along the hole boundary to the applied far-field tensile stress, expressed as $K_t = \frac{\sigma_{max}}{\sigma_0}$. The numerical results for the homogeneous isotropic plate containing a single circular hole were evaluated against the classical Kirsch analytical solution, which

predicts an SCF of 3.0 under uniaxial tensile loading. Relative difference was defined as 100|Kt,num − Kt,ref|/|Kt,ref|. The reported two-hole analysis also used superposition of two single-hole Kirsch fields with subtraction of the duplicated uniform far-field stress; this provides an approximate comparator, not an exact two-hole boundary-value solution. The interaction between adjacent circular holes was evaluated using the normalized center-to-center spacing ratio, λ = s/(2a). The influence of increasing hole separation was assessed by examining changes in the SCF relative to the isolated-hole configuration. The resulting stress concentration factors, numerical comparisons, and stress distributions are presented in the next section.

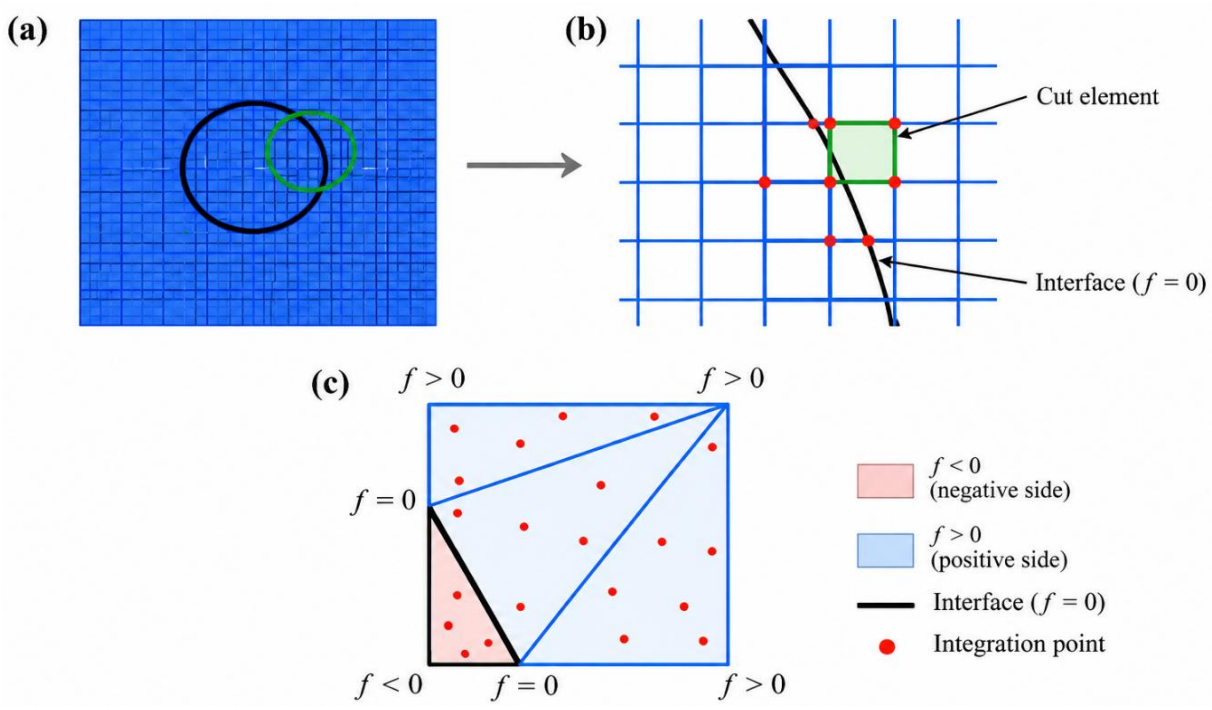


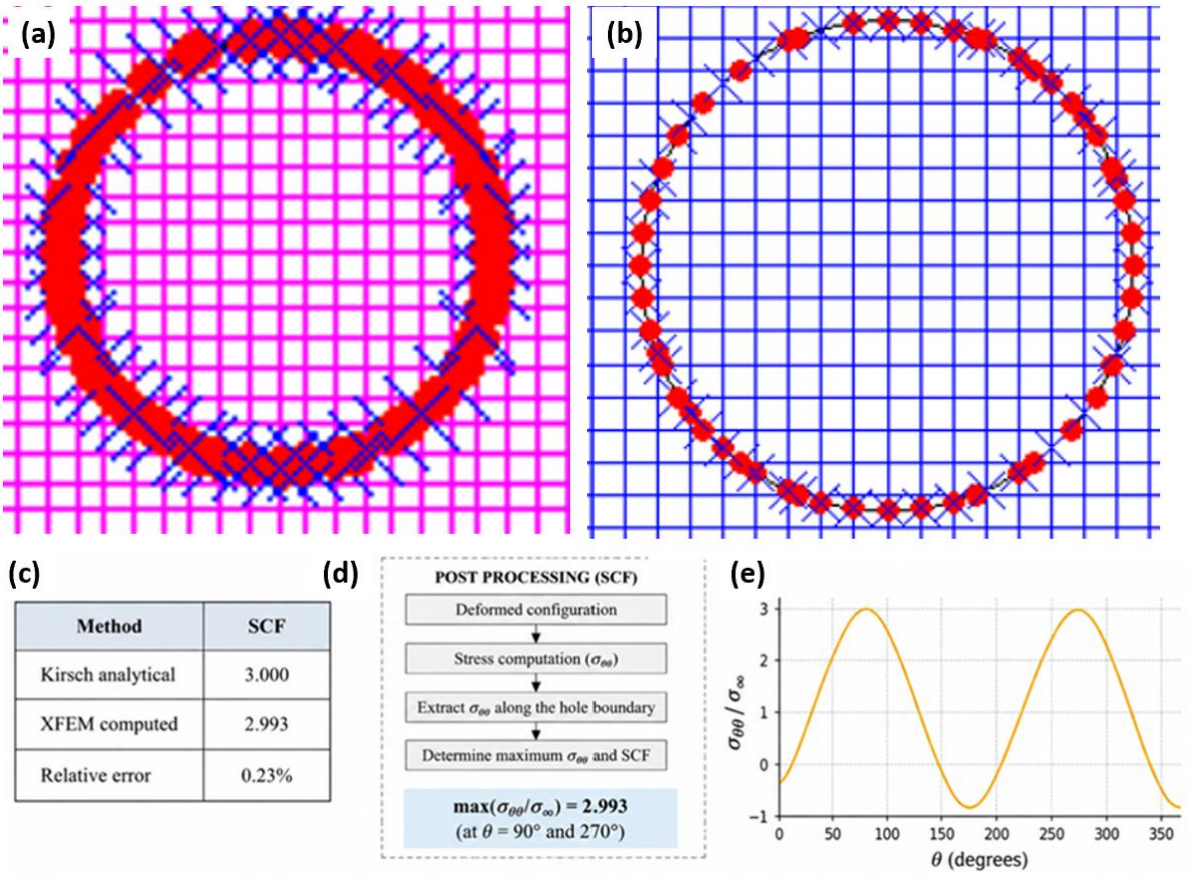
Figure 5. Illustration of the level-set representation and numerical integration in XFEM: (a) computational mesh containing circular interfaces; (b) enlarged view of an element intersected by the level-set boundary; and (c) subdivision of a cut element into triangular integration subdomains, showing the positive and negative level-set regions and integration points.

4. RESULTS AND DISCUSSION

4.1. Numerical Validation for the Isotropic Single-hole Plate

The single circular-hole configuration was examined to evaluate the accuracy of the numerical stress concentration prediction. **Figure 6(a)** illustrates the enriched computational mesh surrounding the circular hole, while **Figure 6(b)** shows the discretized hole boundary and sampling points used for stress evaluation. These representations demonstrate how the XFEM formulation accommodates the circular opening within the computational mesh and identifies locations for evaluating stresses along the hole boundary. The numerical results were evaluated against the classical Kirsch analytical solution for an isotropic plate containing a single circular hole under uniaxial tensile loading. As presented in **Figure 6(c)**, the analytical SCF was 3.000, whereas the XFEM calculation yielded an SCF of 2.993. The absolute difference

was 0.007, corresponding to a relative error of approximately 0.23%. This close agreement indicates that the XFEM formulation reproduces the analytical stress concentration factor with high accuracy for the investigated benchmark configuration. The numerical post-processing procedure is illustrated in **Figure 6(d)**. The procedure involves evaluating the stress field, extracting the circumferential stress along the hole boundary, and determining the maximum stress relative to the applied far-field tensile stress. The resulting SCF of 2.993 is consistent with the numerical validation presented in **Figure 6(c)**. The angular distribution of normalized circumferential stress ($\sigma_{\theta\theta}/\sigma_{\infty}$) is shown in **Figure 6(e)**. The stress distribution exhibits two maxima near θ = 90° and 270°, corresponding to the characteristic circumferential stress concentration around a circular opening under uniaxial tensile loading. The maximum circumferential stress, rather than the average boundary stress, is therefore used to determine the SCF. The agreement between the numerical and analytical results supports the applicability of the XFEM formulation to the single-hole isotropic benchmark. However, the accuracy of the numerical predictions for more complex configurations involving material gradation and interacting circular holes also depends on mesh resolution, enrichment treatment, and numerical integration accuracy. Consequently, the single-hole validation provides a useful reference for interpreting the subsequent parametric investigations but does not independently establish numerical convergence for all investigated configurations.



Method	SCF
Kirsch analytical	3.000
XFEM computed	2.993
Relative error	0.23%

Figure 6. XFEM discretization and numerical validation for an isotropic plate containing a single circular hole: (a) enriched mesh around the hole; (b) boundary discretization and stress evaluation points; (c) comparison of stress concentration factors (SCFs) obtained from the Kirsch analytical solution and XFEM, including the relative error; (d) numerical post-processing

procedure for SCF determination; and (e) angular distribution of normalized circumferential stress ($\sigma_{\theta\theta}/\sigma_{\infty}$) along the hole boundary.

4.2. Influence of Material Gradation on A Single Circular Hole

The influence of material gradation was assessed using the reported gradient indices n = 0, 1, 2, 5, and 10. **Table 1** shows that the SCF increases from 2.51 at n = 0 to 3.56 at n = 10. Intermediate values of 2.78, 3.02, and 3.33 are obtained for n = 1, 2, and 5, respectively. The total change across the investigated range is 1.05, corresponding to approximately 41.8% relative to the value at n = 0. The progressive increase in SCF with the material gradient index demonstrates the influence of spatially varying elastic stiffness on stress concentration around the circular opening. Unlike homogeneous isotropic plates, where the stress distribution is primarily governed by geometry and external loading, FGM plates exhibit additional stress redistribution associated with local variations in mechanical properties. Consequently, the resulting stress concentration depends on both the geometrical configuration and the prescribed material gradation. The corresponding mechanical response depends on the local stiffness distribution and the characteristics of the constituent materials within the functionally graded plate.

Table 1. SCFs for the single-hole FGM plate at different gradient indices.

GRADIENT INDEX (n)	SCF FGM
0 (ceramic-rich)	2.51
1	2.78
2	3.02
5	3.33
10 (metal rich)	3.56

4.3. Interaction between two circular holes in an isotropic plate

The influence of hole interaction was investigated by varying the normalized center-to-center spacing ratio, λ = s/(2a). As shown in **Figure 7(a)**, the reported stress concentration factor (SCF) decreased progressively with increasing hole spacing. At λ = 1.05, the SCF reached 3.88, whereas increasing the spacing ratio to λ = 6.0 reduced the SCF to 3.01. The latter value approached the analytical SCF of 3.0 for an isolated circular hole, indicating that the interaction between adjacent holes weakened as their separation increased. The higher SCF at smaller spacing ratios suggests stronger interaction between the stress fields surrounding the two openings. **Figure 7(b)** presents the numerical post-processing output, including the calculated maximum value of the selected stress component. This output provides information on the numerical stress evaluation; however, interpretation of the reported value requires identification of the stress component, its unit, and the corresponding loading conditions. **Figure 7(c)** compares the normalized circumferential stress distributions obtained from the Kirsch analytical solution for a single hole, the numerical transformation, and the approximate superposition of two-hole stress fields. The superposition approximation produces higher peak circumferential stresses than the single-hole analytical solution, indicating the influence of the neighboring opening on the local stress distribution. Nevertheless, this approximation does not necessarily satisfy the traction-free boundary conditions along both hole boundaries and therefore differs from an exact two-hole elasticity

solution. The influence of normalized hole spacing on the approximate superposition results is further illustrated in **Figure 7(d)**. Unlike the decreasing SCF values reported in Figure 7(a), the SCF predicted by the superposition approach increases gradually with hole spacing and approaches approximately 4.0. The contrasting trends indicate that the two sets of results are not directly equivalent. Their differences may arise from the underlying stress evaluation procedures, normalization assumptions, or locations at which the maximum stress is determined. Consequently, a direct quantitative comparison requires consistent definitions of the SCF and verification of the corresponding computational procedures. The results highlight the importance of distinguishing between numerical stress concentration predictions and approximate analytical representations when evaluating interactions between circular holes.

The combined influence of material gradation and hole spacing is presented in **Figure 8(a)**. At each investigated spacing ratio, the SCF increased with the material gradient index. For λ = 1.05, the SCFs were 3.41, 3.65, and 3.98 for n = 2, 5, and 10, respectively. At λ = 3.0, the corresponding values decreased to 2.94, 3.12, and 3.34. These results indicate that both the spatial distribution of elastic properties and the interaction between adjacent openings influence stress concentration in FGM plates.

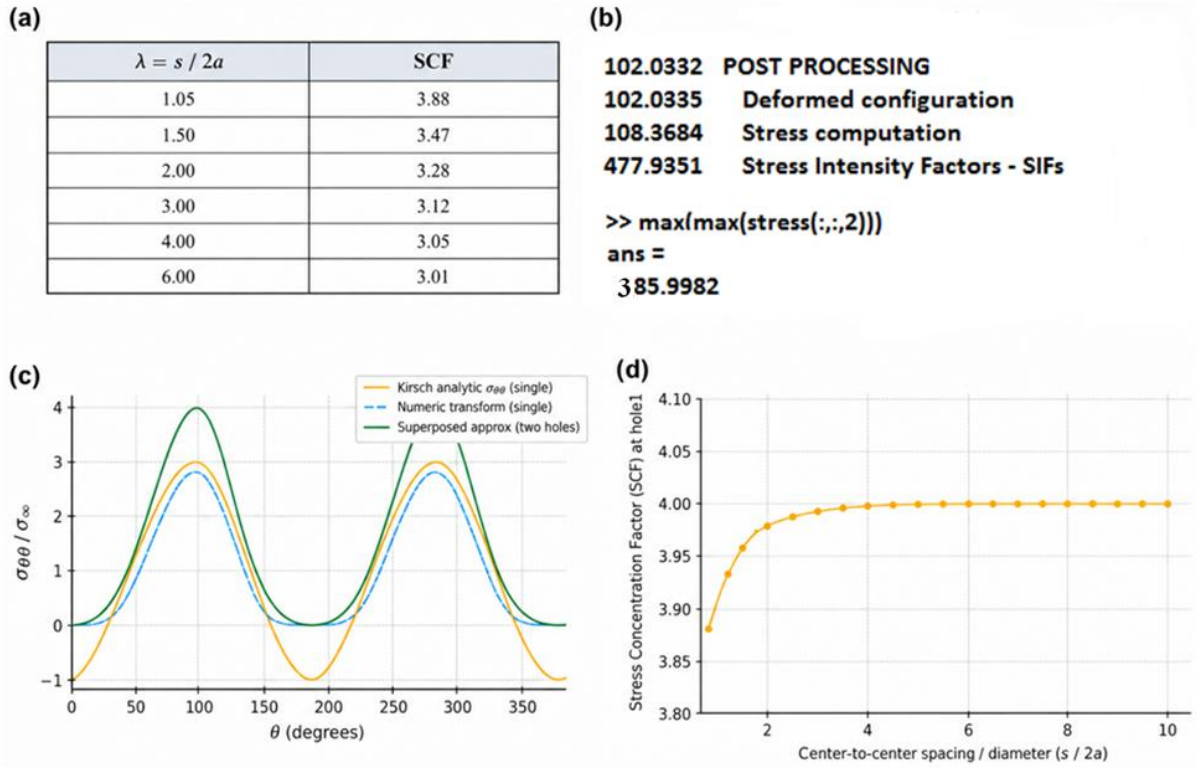


Figure 7. Stress concentration analysis of an isotropic plate containing two circular holes: (a) stress concentration factors (SCFs) at different normalized hole-spacing ratios; (b) numerical post-processing output showing the computed maximum stress; (c) comparison of normalized circumferential stress distributions obtained from the Kirsch analytical solution, numerical transformation, and two-hole superposition approximation; and (d) variation of the SCF at hole 1 with normalized center-to-center spacing based on the approximate superposition method.

4.4. Combined effects of material gradation and hole spacing

At a fixed gradient index, increasing the spacing ratio lowers the SCF (**Figure 8(a)**). For n = 10, the SCF declines from 3.98 at λ = 1.05 to 3.34 at λ = 3.0; for n = 2, the corresponding reduction is from 3.41 to 2.94. Thus, the influence of material gradation persists across the investigated hole spacings, while the magnitude of the hole interaction diminishes as the openings become farther apart. **Figure 8(b)** presents the relationship between the stress concentration factor and the normalized hole diameter-to-plate width ratio (D/W) for a functionally graded plate characterized by the radial elastic-modulus distribution $E_+(r)$. The SCF increases substantially with increasing D/W, indicating greater stress concentration as the opening occupies a larger proportion of the plate width. The XFEM and comparison curves exhibit similar trends over the investigated range, suggesting agreement between the corresponding stress concentration predictions for the radial gradation configuration. This comparison complements the gradient-index analysis in Figure 8(a) by illustrating the influence of hole geometry and spatial variations in elastic stiffness on stress concentration.

4.5. Overall discussion

Stress concentration in perforated plates is influenced by the combined effects of geometrical discontinuities, material gradation, and interactions between adjacent holes. The validation analysis for a homogeneous isotropic plate containing a single circular hole showed close agreement between the XFEM prediction and the classical Kirsch analytical solution. The analytical SCF of 3.000 was reproduced numerically with an SCF of 2.993, corresponding to a relative error of 0.23%. The numerical formulation can accurately capture the dominant stress concentration behavior around an isolated circular opening under the investigated loading conditions. The ability of XFEM to represent geometrical discontinuities independently of a conforming mesh provides an important advantage for analyzing structural components containing holes and inclusions, particularly when conventional finite element discretization becomes geometrically complicated [5, 8].

(a)

λ	SCF (n = 2)	SCF (n = 5)	SCF (n = 10)
1.05	3.41	3.65	3.98
1.50	3.19	3.41	3.67
2.00	3.05	3.25	3.48
3.00	2.94	3.12	3.34

(b)

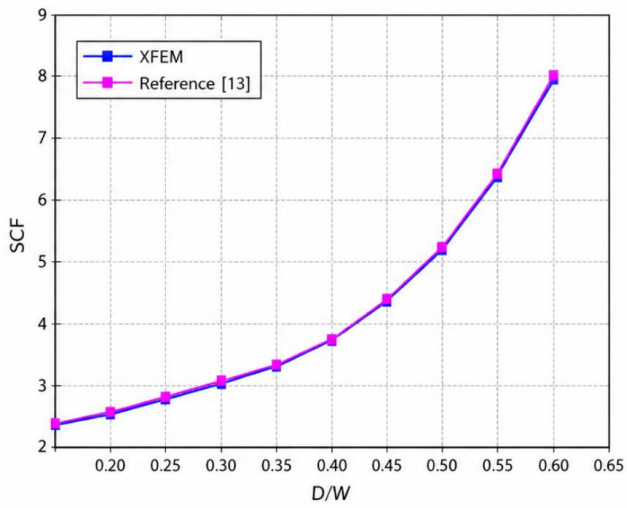


Figure 8. Stress concentration analysis of FGM plates: (a) SCFs for two interacting circular holes at different material gradation indices and spacing ratios; and (b) comparison of XFEM and reference results showing the effect of the normalized hole diameter-to-plate width ratio (D/W) on SCF.

Material gradation substantially influenced the stress concentration behavior of plates containing a single circular hole. Increasing the gradient index from 0 to 10 increased the reported SCF from 2.51 to 3.56, indicating that spatial variations in elastic properties significantly modify local stress distributions. This behavior can be attributed to the redistribution of mechanical stresses arising from differences in local stiffness across the plate. In a homogeneous material, the stress field is governed primarily by geometry and external loading, whereas in an FGM plate, the spatial distribution of elastic modulus introduces an additional factor controlling the mechanical response. Consequently, variations in material gradation can influence both the magnitude and spatial distribution of stresses surrounding a geometrical discontinuity. These observations are consistent with the importance of incorporating material heterogeneity into numerical analyses of functionally graded structures [1, 2, 5].

The interaction between adjacent circular holes introduces additional complexity into the stress concentration behavior. For the investigated isotropic configurations, reducing the normalized spacing ratio increased the reported SCF from 3.01 at λ = 6.0 to 3.88 at λ = 1.05. Closely spaced holes produce stronger stress interactions than widely separated openings. When the holes are sufficiently separated, the stress disturbances associated with each opening become less influential on the neighboring hole, and the resulting SCF approaches the isolated-hole reference value. Conversely, decreasing the spacing causes the stress fields surrounding adjacent openings to interact more strongly, increasing the local concentration of mechanical stresses. The approximate two-hole superposition analysis further illustrates the sensitivity of circumferential stress distributions to the presence of neighboring openings. However, because analytical superposition does not generally satisfy the complete traction-free boundary conditions at both interacting holes, its predictions should be distinguished from those obtained directly through numerical simulation.

The simultaneous effects of material gradation and hole spacing were also evident in the FGM configurations. At the smallest investigated spacing ratio, λ = 1.05, increasing the gradient index from 2 to 10 increased the SCF from 3.41 to 3.98. At λ = 3.0, the corresponding

SCFs ranged from 2.94 to 3.34. The influence of material gradation remains significant across different geometrical configurations. The increased stress concentration associated with higher gradient indices suggests that local stiffness variations can intensify the mechanical response around interacting openings. Meanwhile, increasing the spacing ratio consistently reduced the SCF for each investigated gradient index. Therefore, material gradation and hole spacing should not be considered independently when assessing the mechanical performance of perforated FGM plates. Their combined influence determines the local stress concentration and may affect the selection of material-property distributions and opening arrangements for structural applications [5, 7].

The results also highlight the significance of accurately representing geometrical boundaries and evaluating numerical stresses near discontinuities. The level-set formulation enables circular openings to be described independently of the computational mesh, while XFEM enrichment provides a flexible framework for handling embedded boundaries and discontinuous fields. These characteristics are particularly useful for analyzing geometrical configurations involving multiple holes or spatially varying material properties. Nevertheless, the numerical accuracy of enriched finite element formulations is influenced by the selection of enrichment functions, numerical integration procedures, and discretization characteristics. Appropriate treatment of intersected elements and integration subdomains is therefore essential for reliable stress evaluation [8, 12].

From an engineering perspective, stress concentration in perforated FGM plates can be influenced through both material-property distribution and geometrical configuration. Increasing the separation between adjacent holes reduces their mechanical interaction, while changes in material gradation may either increase or decrease local stress concentration depending on the prescribed gradation profile. These considerations are relevant to the numerical assessment of lightweight structural components, perforated mechanical parts, and graded plates containing functional openings. However, the agreement obtained for the isolated-hole benchmark does not establish convergence for every FGM and two-hole configuration. Further evaluation of mesh refinement, integration accuracy, and alternative gradation profiles would strengthen the quantitative assessment of the numerical predictions. The development of enrichment-based finite element formulations has demonstrated the flexibility of XFEM for representing geometrical discontinuities and complex crack configurations without requiring the mesh to conform to the discontinuity geometry [13]. The results demonstrate the usefulness of combining XFEM with level-set boundary representation for investigating stress concentration in geometrically discontinuous materials, while emphasizing the need to distinguish validated numerical predictions from approximate analytical comparisons [8, 12].

5. CONCLUSION

The numerical investigation examined stress concentration around circular holes in isotropic and functionally graded plates using an extended finite element framework. For the isotropic single-hole benchmark, the reported numerical SCF closely matched the classical analytical value. Material gradation altered the stress concentration substantially, with larger gradient indices producing higher reported values. In two-hole configurations, decreasing the distance between openings increased stress amplification, whereas widely separated holes approached isolated-hole behavior. Combined gradation and spacing analyses demonstrated that geometry and spatial stiffness variation jointly influence local stress responses. These findings support careful consideration of both parameters in perforated plate design.

6. ACKNOWLEDGMENTS

This study acknowledges Nam Can Tho University, Viet Nam.

7. AUTHORS' NOTE

The authors declare that there is no conflict of interest regarding the publication of this article. The authors confirm that the paper was free of plagiarism.

8. REFERENCES

[1] Cavaliere, P., Cerri, E., and Leo, P. (2004). Hot deformation and processing maps of a particulate reinforced 2618/Al2O3/20p metal matrix composite. *Composites Science and Technology*, *64*(9), 1287-1291.

[2] Praveen, G. N., and Reddy, J. N. (1998). Stress analysis of functionally graded plates using the first-order shear deformation theory. *Composite Structures*, *43*, 333-349.

[3] Nandiyanto, A. B. D., Triawan, F., Firly, R., and Kishimoto, K. (2021). Crystallite size on micromechanical characteristics of WO3 microparticles. *Journal of Engineering Research*, *9*(3), 268-277.

[4] Nandiyanto, A. B. D., Triawan, F., Firly, R., Abdullah, A. G., Aono, Y., Inaba, K., and Kishimoto, K. (2019). Identification of micro-mechanical characteristics of monoclinic tungsten trioxide microparticles by nanoindentation technique. *Materials Physics and Mechanics*, *42*(3), 323-329.

[5] Singh, I. V., Mishra, B. K., and Bhattacharya, S. (2011). XFEM simulation of cracks, holes and inclusions in functionally graded materials. *International Journal of Mechanics and Materials in Design*, *7*(3), 199-218.

[6] Nguyen, H. D., and Huang, S. C. (2023). Use of XTFEM based on the consecutive interpolation procedure of quadrilateral element to calculate J-integral and SIFs of an FGM plate. *Theoretical and Applied Fracture Mechanics*, *127*, 103985.

[7] Nguyen, D. H. (2025). XFEM simulation of functionally graded plates with arbitrary openings. *VNUHCM Journal of Science and Technology Development*, *28*(4), 3870-3877.

[8] Sukumar, N., Chopp, D. L., Moës, N., and Belytschko, T. (2001). Modeling holes and inclusions by level sets in the extended finite-element method. *Computer methods in applied mechanics and engineering*, *190*(46-47), 6183-6200.

[9] Belytschko, T., and Black, T. (1999). Elastic crack growth in finite elements with minimal remeshing. *International journal for numerical methods in engineering*, *45*(5), 601-620.

[10] Moës, N., Dolbow, J., and Belytschko, T. (1999). A finite element method for crack growth without remeshing. *International Journal for Numerical Methods in Engineering*, *46*(1), 131-150.

[11] Daux, C., Moës, N., Dolbow, J., Sukumar, N., and Belytschko, T. (2000). Arbitrary branched and intersecting cracks with the extended finite element method. *International Journal for Numerical Methods in Engineering*, *48*(12), 1741-1760.

[12] Sukumar, N., and Prévost, J. H. (2003). Modeling quasi-static crack growth with the extended finite element method Part I: Computer implementation. *International Journal of Solids and Structures*, *40*(26), 7513-7537.

[13] Sukumar, N., Moës, N., Moran, B., and Belytschko, T. (2000). Extended finite element method for three-dimensional crack modelling. *International journal for numerical methods in engineering*, *48*(11), 1549-1570.